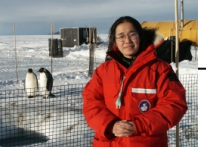

Lecture 13. Temperature Lidar (2) Integration Techniques

- Introduction
- Integration technique for temperature
  - Searchlight integration lidar
  - Falling sphere temperature measurement
  - Rayleigh integration temperature lidar
  - Vibrational-rotational Raman integration lidar
- Rayleigh/Raman lidar instrumentation
- Non-integration techniques near boundary layers
  - Pure-rotational-Raman Boltzmann lidar
  - Vibrational-rotational-Raman Doppler lidar
- Summary

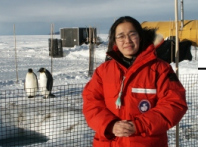

Introduction: Temperature Measurements in Atmospheric Lidars

Use temperature-dependent/sensitive effects or phenomena

- Doppler Technique - Doppler broadening of radiation spectrum caused by thermal motions (not only for Fe, Na, and K etc. atomic absorption, but also for Rayleigh scattering, Raman scattering, and molecular absorption, as long as Doppler broadening dominate and can be detected)
- Boltzmann Technique - Boltzmann distribution of atomic/molecular populations on different energy levels under thermodynamic equilibrium (not only for Fe atomic absorption, but also for Raman scattering, molecular absorption, and airglow in optical remote sensing)
- Integration Technique (Rayleigh or Raman) - integration lidar technique using ideal gas law and assuming hydrostatic equilibrium (not only for modern lidar, but also for cw searchlight and rocket falling sphere - some way to measure atmosphere number density)

Each technique can be applied to various physical processes, and the complexity of lidar instrumentation varies significantly with these different techniques or physical processes involved.

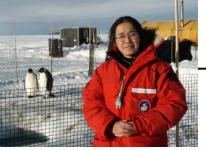

Introduction: Doppler & Boltzmann

- Doppler effect and Boltzmann distribution are two effects that are directly temperature-dependent. The Doppler technique and Boltzmann technique are "straight-forward" in the sense of deriving temperature or wind. However, the lidar architecture is usually complicated and sophisticated, due to the high demands on frequency accuracy and tuning, laser linewidth, and laser power, etc.

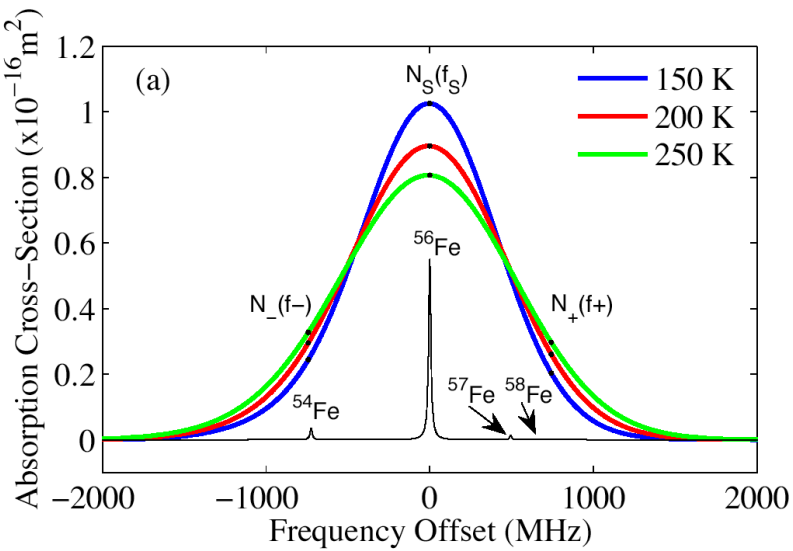

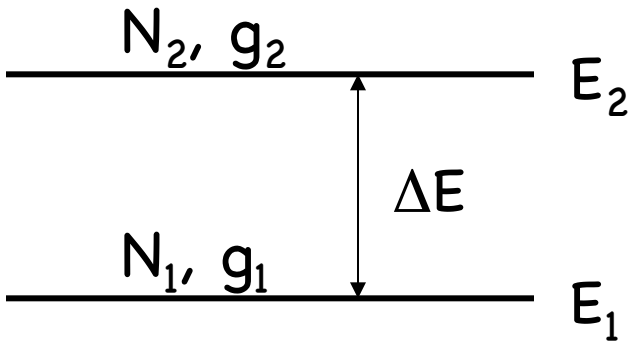

$$\frac{N_2}{N_1} = \frac{g_2}{g_1}\exp\left\{-\left(E_2 - E_1\right)/k_B T\right\}$$

$$\Delta\omega = \omega - \omega_0 = -\vec{k}\cdot\vec{v} = -\omega_0 \frac{v\cos\theta}{c}$$

$$\sigma_{rms} = \frac{\nu_0}{c}\sqrt{\frac{k_B T}{M}} = \frac{1}{\lambda_0}\sqrt{\frac{k_B T}{M}}$$

$$T = \frac{\Delta E / k_B}{\ln\left(\frac{g_2}{g_1}\cdot\frac{N_1}{N_2}\right)}$$

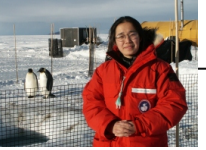

Introduction: Integration Technique

- Integration technique is to utilize the ideal gas law and hydrostatic equation to derive atmospheric temperatures from relative number density (i.e., number density ratio) if a seeding temperature is given. The Rayleigh integration lidar architecture is much simpler than Doppler and Boltzmann lidars. Basically every lidar can act as a Rayleigh integration lidar.

Hydrostatic Equation

$$dP = -\rho g dz$$

+

Ideal Gas Law

$$P = \rho R T$$

$$T(z) = T(z_o)\frac{\rho(z_o)}{\rho(z)} + \frac{1}{R}\int_z^{z_o} g(r)\frac{\rho(r)}{\rho(z)}dr$$

Seeding Temperature

Relative Density

$T(z_0)$ - Seeding Temperature; ρ - number density
R - gas constant for dry air; g - gravitational acceleration

Number Density Ratio ⇒ Temperature
(lidar backscatter ratio at different altitudes)

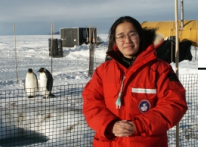

Integration Technique

- The hydrostatic equation $$\boxed{\mathrm{d}P(z) = -\rho(z)g(z)\mathrm{d}z}$$
- Ideal gas law $$\boxed{P(z) = \frac{\rho(z)RT(z)}{M(z)}}$$
- Integration from the upper altitude yields

$$\boxed{T(z) = T(z_0)\frac{\rho(z_0)}{\rho(z)}\frac{M(z)}{M(z_0)} + \frac{M(z)}{R}\int_z^{z_0}\frac{\rho(z')g(z')}{\rho(z)}\mathrm{d}z'}$$

$T(z)$ = atmospheric temperature profile (K)

$P(z)$ = atmospheric pressure profile (mbar)

$\rho(z)$ = atmospheric mass density profile (kg/m^3)

$g(z)$ = gravitational acceleration (m/s^2)

$M(z)$ = mean molecular weight of the atmosphere, i.e., molecular mass per mole (kg/mol)

R = universal gas constant (8.314472 J/mol/K)

z_0 = altitude of the upper level starting temperature (m)

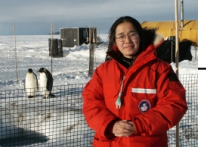

Integration Technique

- Atmosphere mass density *ρ(z)* vs number density *n(z)*

$$\rho(z) = n(z)M(z)/N_A$$

where N_A is the Avogadro constant: $N_A = 6.02214179 \times 10^{23}\ \mathrm{mol}^{-1}$

- Thus, we have

$$T(z) = T(z_0)\frac{n(z_0)}{n(z)} + \frac{M(z)}{R}\int_z^{z_0} \frac{n(z')M(z')g(z')}{n(z)M(z)}\,\mathrm{d}z'$$

- Below 100 km for the well-mixed atmosphere, we have M(z) = M(z'), so they cancel out in the integration

$$T(z) = T(z_0)\frac{n(z_0)}{n(z)} + \frac{M(z)}{R}\int_z^{z_0} \frac{n(z')g(z')}{n(z)}\,\mathrm{d}z'$$

- Number density ratio (relative number density)

⇨ Temperature profile

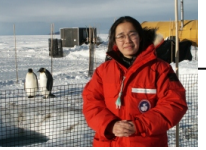

Error Analysis for Integration Tech

- The uncertainty is determined by the photon noise and upper altitude temperature $T(z_0)$. The variance of derived temperature is given by

$$\mathrm{var}[T(z)] \approx \frac{T^2(z)}{N_R(z)} + \left\{ \mathrm{var}[T(z_0)] + \frac{T^2(z_0)}{N_R(z_0)} \right\} \exp[-2(z_0 - z)/H]$$

- After 1-2 scale height, the error introduced by $T(z_0)$ is not important anymore. So the temperature error is mainly determined by the photon counts and their noise.

- The key is how to measure atmosphere (relative) density with high accuracy and precision. Different approaches can be applied, not limited to pulsed lidar technique (as shown in the next slide).

- A major issue of pulsed Rayleigh lidar is the saturation of photo detector over a very large dynamic range – causing systematic bias (inaccuracy). Another issue is that a Rayleigh lidar runs out of signals quickly with increasing altitudes (imprecision). It's very hard for Rayleigh lidars to get good temperatures above 80 km at high resolutions.

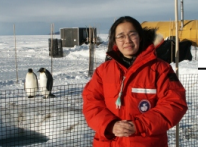

From CW Searchlight to Rayleigh and Raman Lidars as well as Rocket Falling Sphere

- Integration temperature technique relies on the assumptions of hydrostatic equilibrium equation and ideal gas law in atmosphere. It involves integrating the atmosphere relative density profile downward using a starting temperature at an upper altitude.
- It was pioneered by *Elterman* [1951, 1953, 1954] with cw searchlight to measure stratospheric density thus deriving temperature in 1950s.
- The use of high power lasers with the Rayleigh lidar in the atmosphere region (30-100 km) free of aerosol and fluorescence was pioneered by *Hauchecorne and Chanin* [1980] (French group).
- In the lower atmosphere where aerosol scattering contaminates Rayleigh scattering, *Keckhut et al.* [1990] developed Raman lidar to measure atmosphere density from vibrational Raman scattering and then derive temperature below 30 km.
- Inflatable falling sphere provides high-precision atmosphere density thus temperature measurements [*Schmidlin et al.,* 1991].

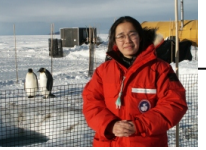

Rayleigh, Raman & Falling Sphere using Integration Temperature Technique

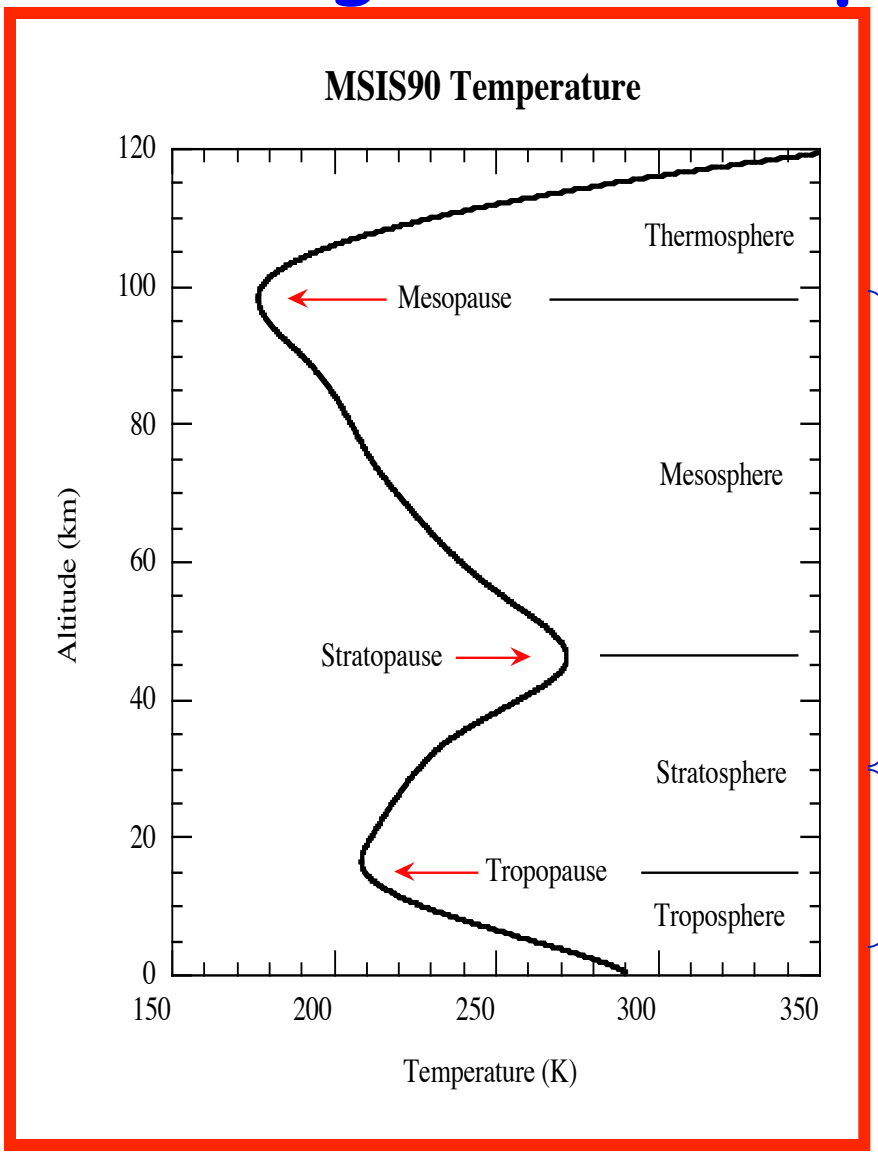

Rayleigh Integration Lidar

Vibrational Raman Lidar

Falling Sphere

Searchlight

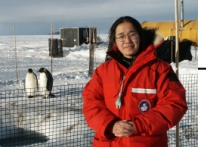

Searchlight Integration Lidar

$$I_{scatter} \propto n_{atmos}$$

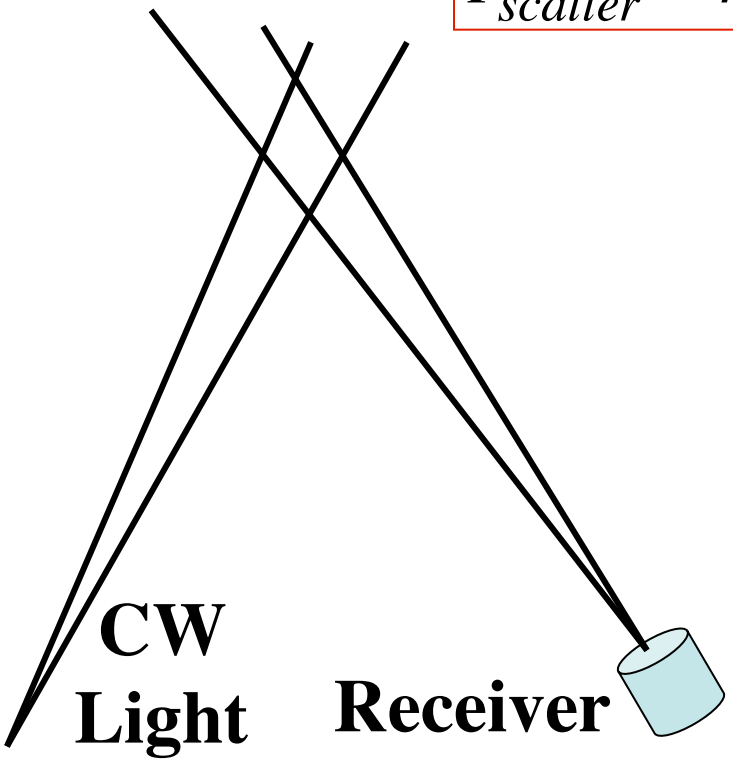

Bistatic Configuration

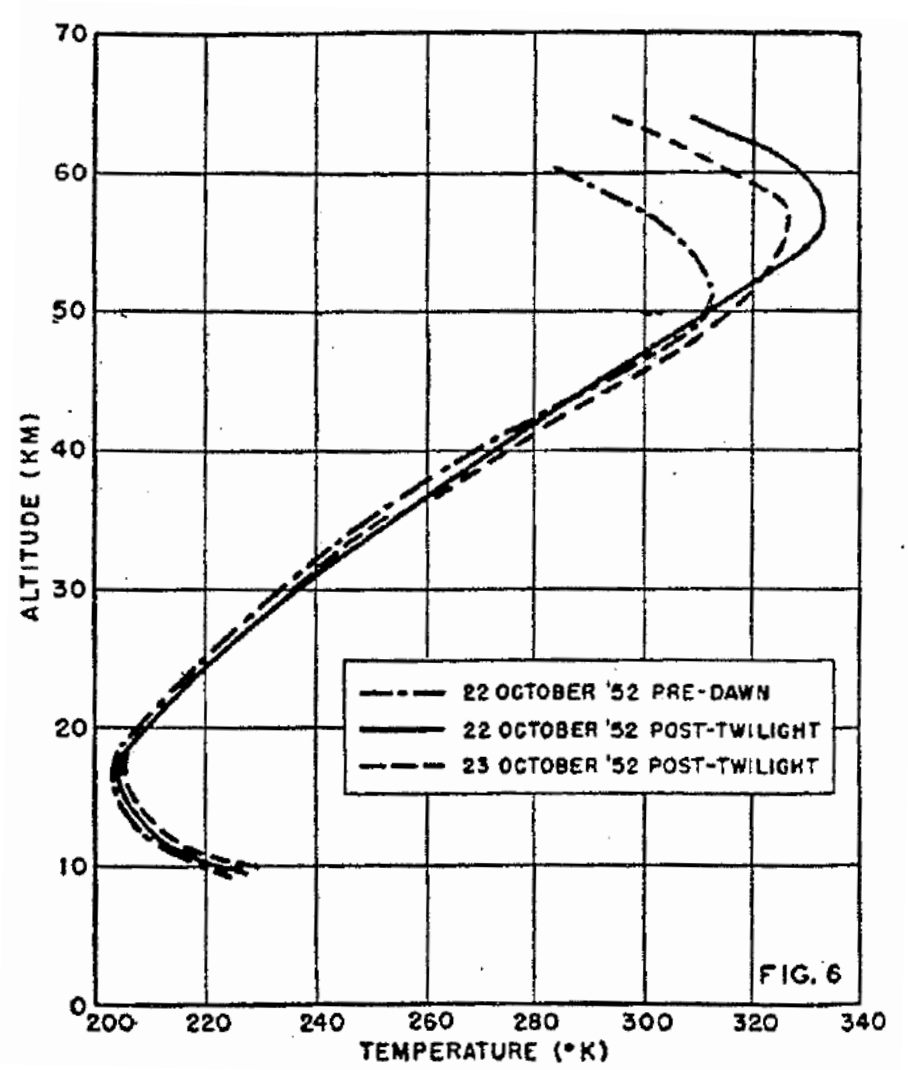

[Elterman, JGR, 1954]

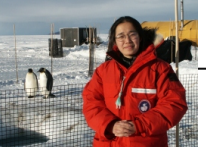

Inflatable Falling Sphere

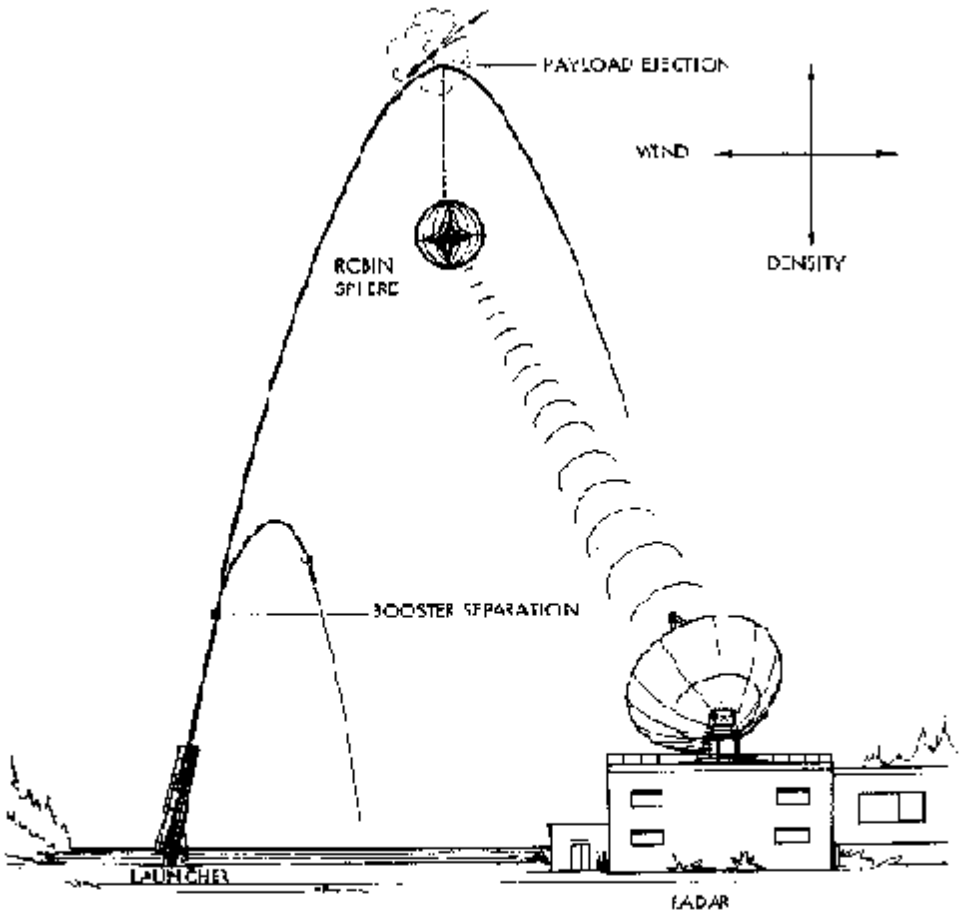

SPACE DATA CORPORATION

Bollerman and Walker, 1983

Rocket transports a metal sphere to upper atmosphere

⇩

After release the sphere inflates to 1-m metal sphere falling through atmosphere

⇩

High-precision radar tracks sphere position & acceleration

⇩

Input to the equation of motion of the falling sphere to derive atmosphere density

⇩

Integration from top to derive temperature from density data

[Schmidlin et al., JGR, 96(D12), 22673-22682, 1991]

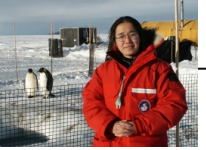

Falling Sphere Temperature

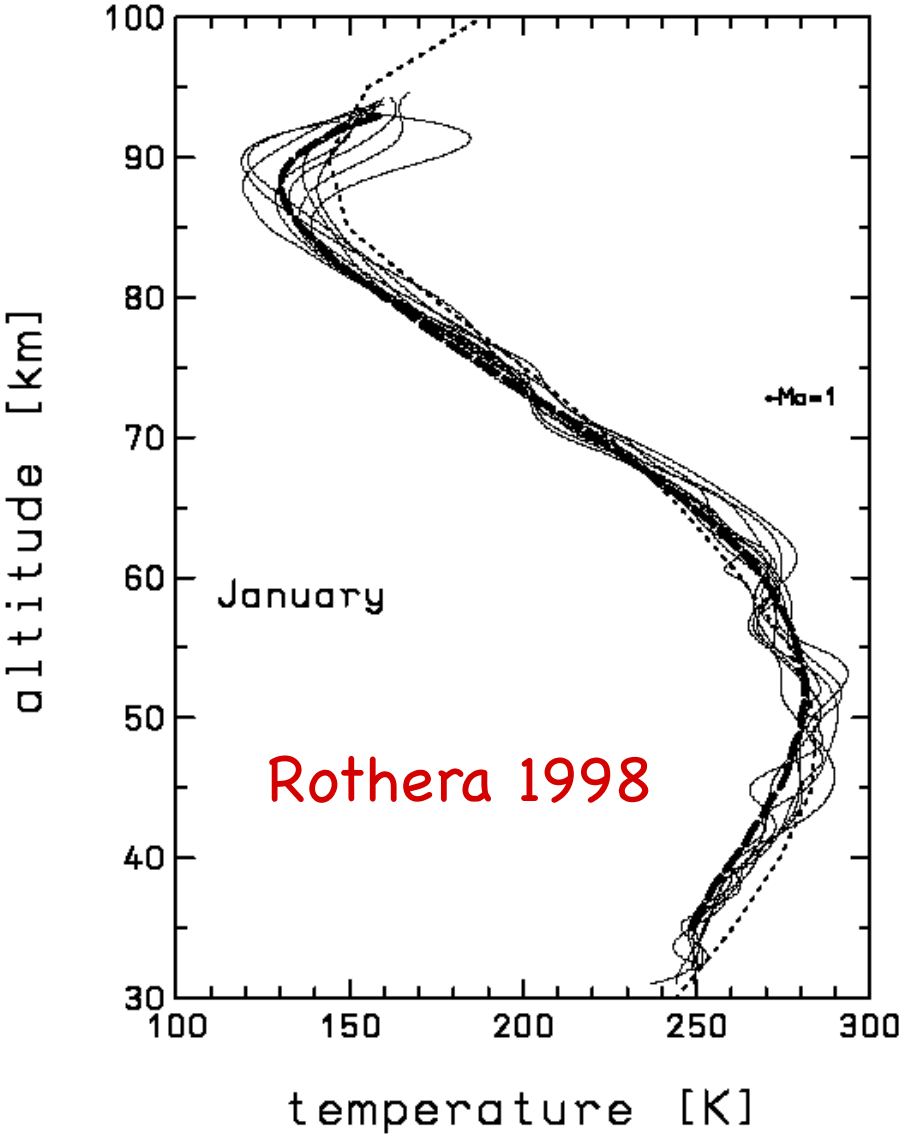

[Lübken et al., GRL, 1999]

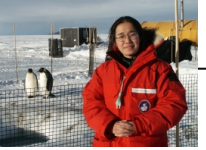

Rayleigh Integration Lidar

- In the atmosphere region free of aerosols and fluorescence, the lidar return photon counts are given by

$$N_S(\lambda,z) = \left(\frac{P_L(\lambda)\Delta t}{hc/\lambda}\right)\left(\beta_{Rayleigh}(z)\Delta z\right)\left(\frac{A}{z^2}\right)T_a^{\,2}(\lambda,z)\left(\eta(\lambda)G(z)\right) + N_B$$

where Rayleigh backscatter coefficient is proportional to atmosphere number density

$$\beta_{Ray}(z) = \sigma_{Ray}(\pi,\lambda)n_a(z)$$

- Thus, the ratio of normalized photon counts gives the atmosphere relative density information

$$\frac{N_S(z_1) - N_B}{N_S(z_2) - N_B}\frac{z_1^2}{z_2^2} = \frac{n_a(z_1)}{n_a(z_2)}$$

Note that T_a^2 caused by lower atmosphere attenuation has been cancelled out by taking signal ratios between different altitudes z_1 and z_2 or by Rayleigh normalization.

Lidar Backscatter Ratio ⇨ Relative Density ⇨ Temperature
(at different altitudes) (Rayleigh)

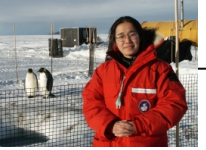

Sample of Temperature and Error

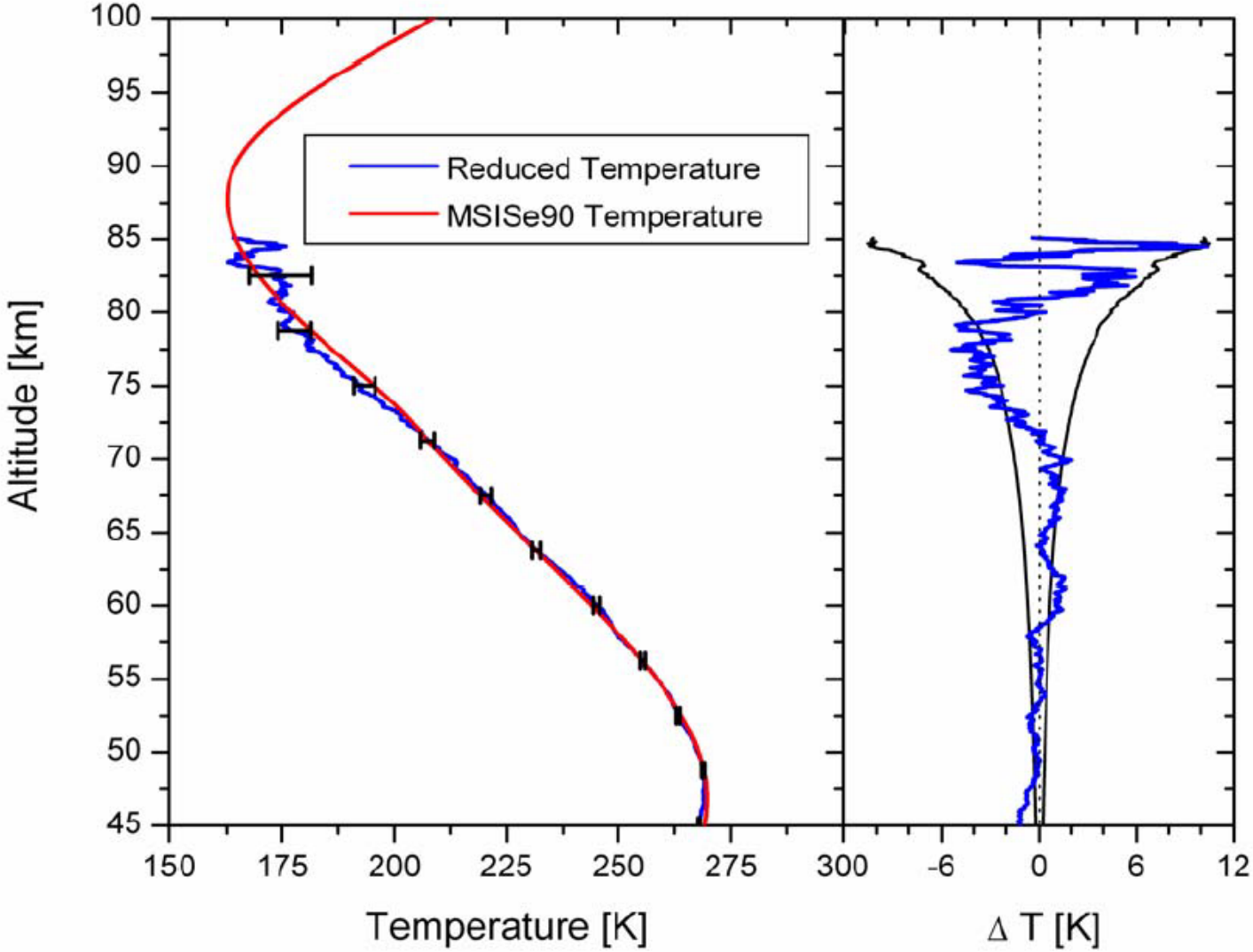

Courtesy of Josh Herron and Prof. Vincent Wickwar @ USU

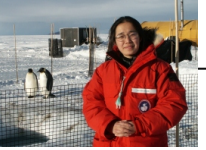

Aerosol Contamination to Rayleigh Sig

- In the atmosphere when aerosols present, the lidar returns contains a narrow spike near the laser frequency caused by aerosol scattering riding on a Doppler broadened molecular scattering profile.

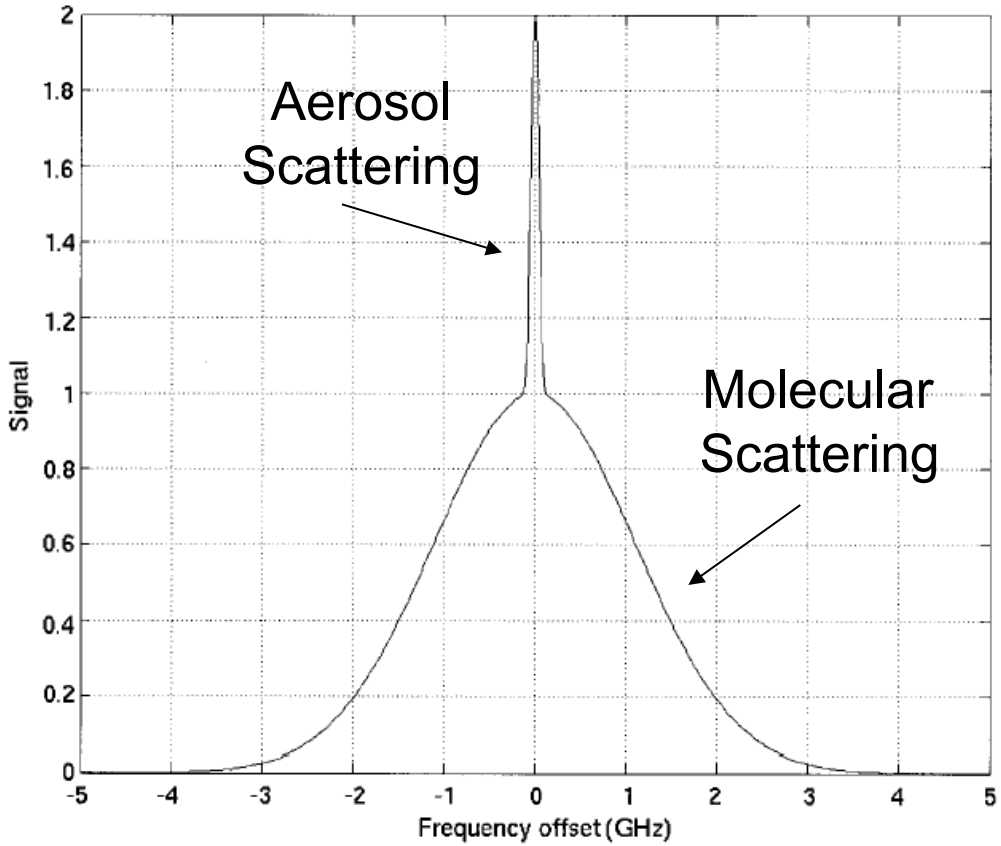

Fig. 5.1. Spectral profile of backscattering from a mixture of molecules and aerosols for a temperature of 300 K. The spectral width of the narrow aerosol return is normally determined by the line width of the transmitting laser.

- Rayleigh integration lidar is broadband so doesn't analyze the return spectra. Thus, all signals will be detected (or photo counted). Thus, the aerosol elastic scattering contaminates the Rayleigh elastic scattering (sharing the same wavelength), which no long obeys the ideal gas law.
- Therefore, pure Rayleigh integration lidar cannot work in the region with aerosols.

Courtesy of Dr. Ed Eloranta

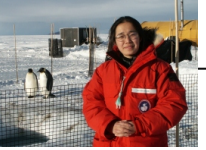

For Regions Not-Free-of-Aerosols

- Elastic scattering from air molecules and aerosols

$$N_S(\lambda,z) = \left(\frac{P_L(\lambda)\Delta t}{hc/\lambda}\right)\left(\beta_{Ray}(z) + \beta_{aer}(z)\right)\Delta z\left(\frac{A}{z^2}\right)\exp\left[-2\int_0^z\left(\alpha_{aer}(z')\right)dz'\right]\exp\left[-2\int_0^z\left(\alpha_{Ray}(z')\right)dz'\right]\left(\eta(\lambda)G(z)\right) + N_B$$

Rayleigh scattering — Aerosol scattering — Aerosol extinction — Rayleigh extinction

- Aerosol contamination makes the elastic scattering signals deviated from the ideal gas properties → Rayleigh integration technique cannot be applied to regions with aerosols.

- Inelastic scattering – Raman scattering from air molecules

$$N_S(\lambda,\lambda_L,z) = \left(\frac{P_L(\lambda_L)\Delta t}{hc/\lambda_L}\right)\left(\sigma_{Raman}(\lambda_L,\lambda,z)n_{N_2}(z)\Delta z\right) \times\left(\frac{A}{z^2}\right)T_a(\lambda_L,z)T_a(\lambda,z)\left(\eta(\lambda_L)\eta(\lambda)G(z)\right) + N_B$$

- The backscattering signal β is free of aerosol contamination, but aerosol extinction is still included in the T_a part.

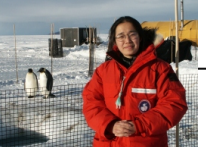

Raman Scattering of N_2 and O_2

532 nm

607 nm

355 nm

387 nm

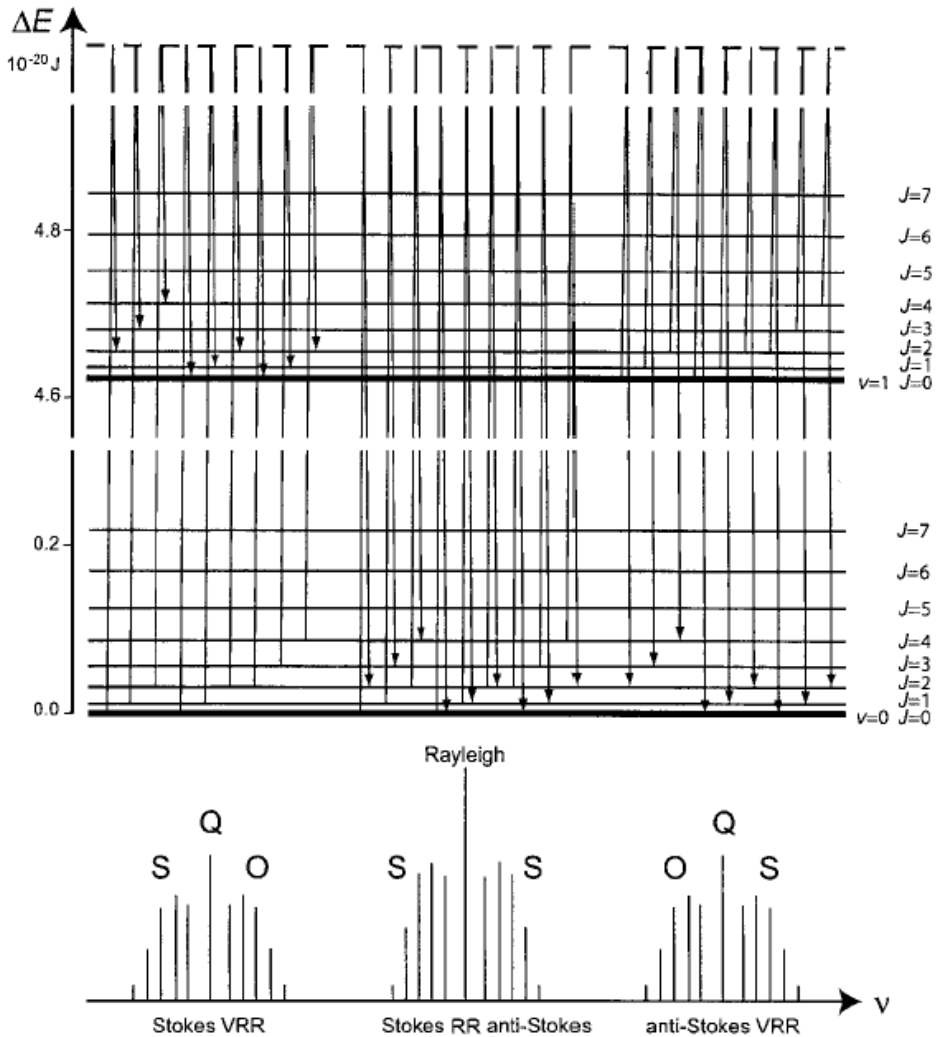

Fig. 9.1. Vibration–rotation energy levels of the N_2 molecule, Raman transitions, and resulting spectrum.

- Raman shift amount is independent of incident laser wavelength

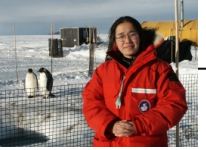

VR Raman Integration Lidar

- In the lower atmosphere region where aerosols present Rayleigh scattering returns are contaminated by aerosol scattering, so cannot be used in the integration technique.
- However, Raman scattering only comes from molecules, thus, free of aerosol influence. By detecting Raman scattering at a different wavelength (e.g., 607 nm compared to 532 nm), Mie and Rayleigh contaminations in the backscattering signals are avoided.

$$N_S(\lambda,\lambda_L,z) = \left(\frac{P_L(\lambda_L)\Delta t}{hc/\lambda_L}\right)\left(\sigma_{Raman}(\lambda_L,\lambda,z)n_{N_2}(z)\Delta z\right) \times\left(\frac{A}{z^2}\right)T_a(\lambda_L,z)T_a(\lambda,z)\left(\eta(\lambda_L)\eta(\lambda)G(z)\right)+N_B$$

- Vibrational-rotational Raman integration works in the regions that aerosols are not too strong and not varying too much.

Lidar Backscatter Ratio ⇨ Relative Density ⇨ Temperature
(at different altitudes) (Raman)

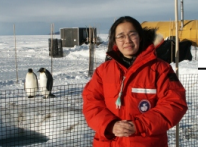

Rayleigh-Raman Integration Lidar

[Keckhut et al., 1990]

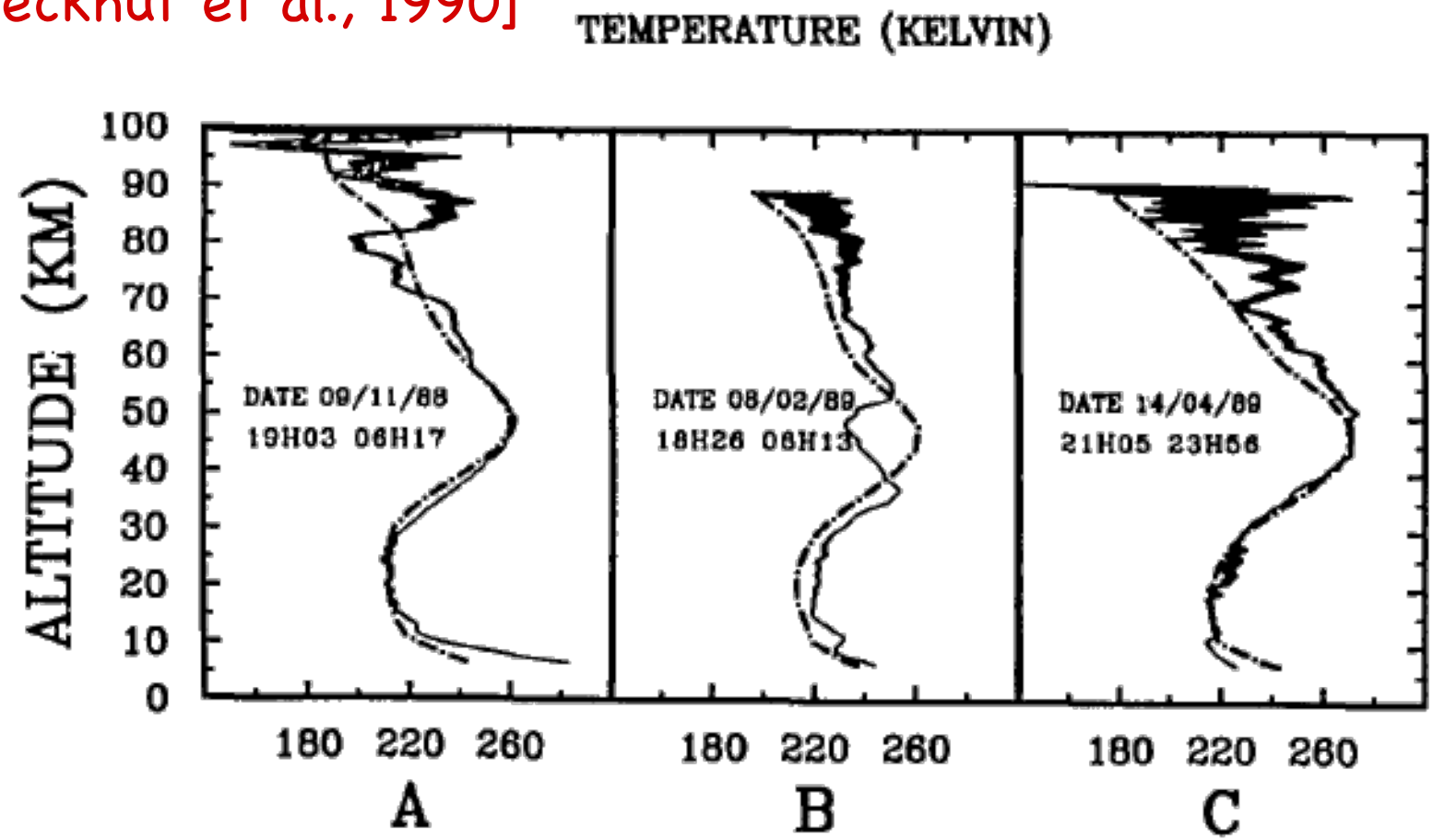

Fig. 2. Lidar temperature profiles compared with the corresponding CIRA 1988 model (dashed lines): (A) 09/11/88, 19H03 06H17; (B) 08/02/89, 18H26 06H13; (C) 14/04/89, 21H05 23H56.

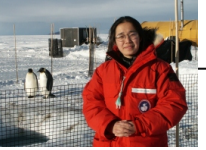

For Regions Near Boundary Layers

- Inelastic scattering – Raman scattering from air molecules

$$N_S(\lambda,\lambda_L,z) = \left(\frac{P_L(\lambda_L)\Delta t}{hc/\lambda_L}\right)\left(\sigma_{Raman}(\lambda_L,\lambda,z)n_{N_2}(z)\Delta z\right)\left(\frac{A}{z^2}\right)$$
$$\times\exp\left[-\int_0^z\left(\alpha_{aer}(\lambda_L,z')\right)dz'\right]\exp\left[-\int_0^z\left(\alpha_{aer}(\lambda,z')\right)dz'\right]$$
$$\times\exp\left[-\int_0^z\left(\alpha_{Ray}(\lambda_L,z')\right)dz'\right]\exp\left[-\int_0^z\left(\alpha_{Ray}(\lambda,z')\right)dz'\right]$$
$$\times\left(\eta(\lambda_L)\eta(\lambda)G(z)\right)+N_B$$

- Aerosol extinction effects cannot be cancelled out between different altitudes when aerosols dominate and vary dramatically with altitude.

$$\frac{N_S(z_1)-N_B}{N_S(z_2)-N_B}\frac{z_1^2}{z_2^2} = \frac{n_{N_2}(z_1)}{n_{N_2}(z_2)}\cdot\frac{\exp\left[-\int_0^{z_1}\left(\alpha_{aer}(\lambda_L,z')\right)dz'\right]\exp\left[-\int_0^{z_1}\left(\alpha_{aer}(\lambda,z')\right)dz'\right]}{\exp\left[-\int_0^{z_2}\left(\alpha_{aer}(\lambda_L,z')\right)dz'\right]\exp\left[-\int_0^{z_2}\left(\alpha_{aer}(\lambda,z')\right)dz'\right]}$$

- Consequently, VR Raman usually does not work below 5 km, especially near the planetary boundary layers.

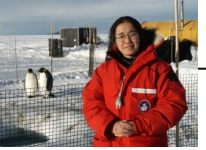

Rayleigh & VR Raman Integration Lidar Instrumentation

- Typical Rayleigh and vibrational-rotational Raman temperature lidar utilizes the commercial Nd:YAG laser system as it provides robust laser power and operation (usually broadband).
- Any (short wavelength) resonance fluorescence lidar, like Fe Boltzmann lidar, also functions as a Rayleigh lidar in the region free of aerosol and fluorescence (about 30-75 km).
- Rayleigh scattering is inversely proportion to the 4th power of wavelength. So the shorter the wavelength, the stronger the Rayleigh scattering, as long as atmosphere absorption is not too strong. Also, 355 nm is regarded as eye-safe region than 532 nm.
- Operating in deep Fraunhofer lines will benefit daytime operation to reduce the solar background.
- Availability and robustness of laser systems are another consideration in lidar design.

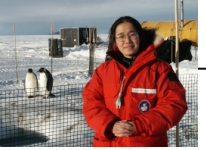

Fe Boltzmann/Rayleigh Lidar

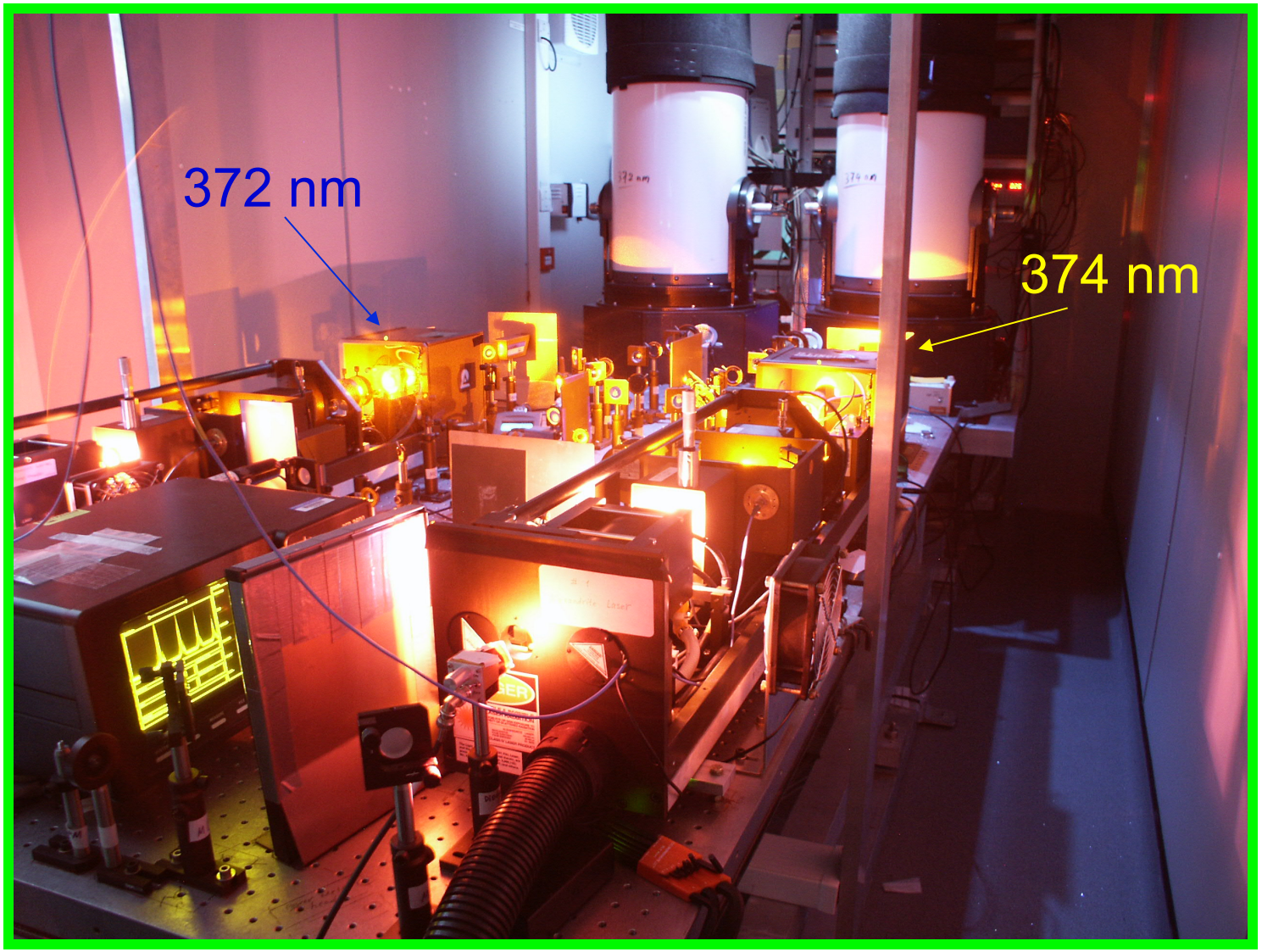

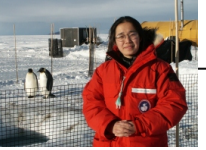

Sample Results from Fe Boltzmann/Rayleigh Lidar

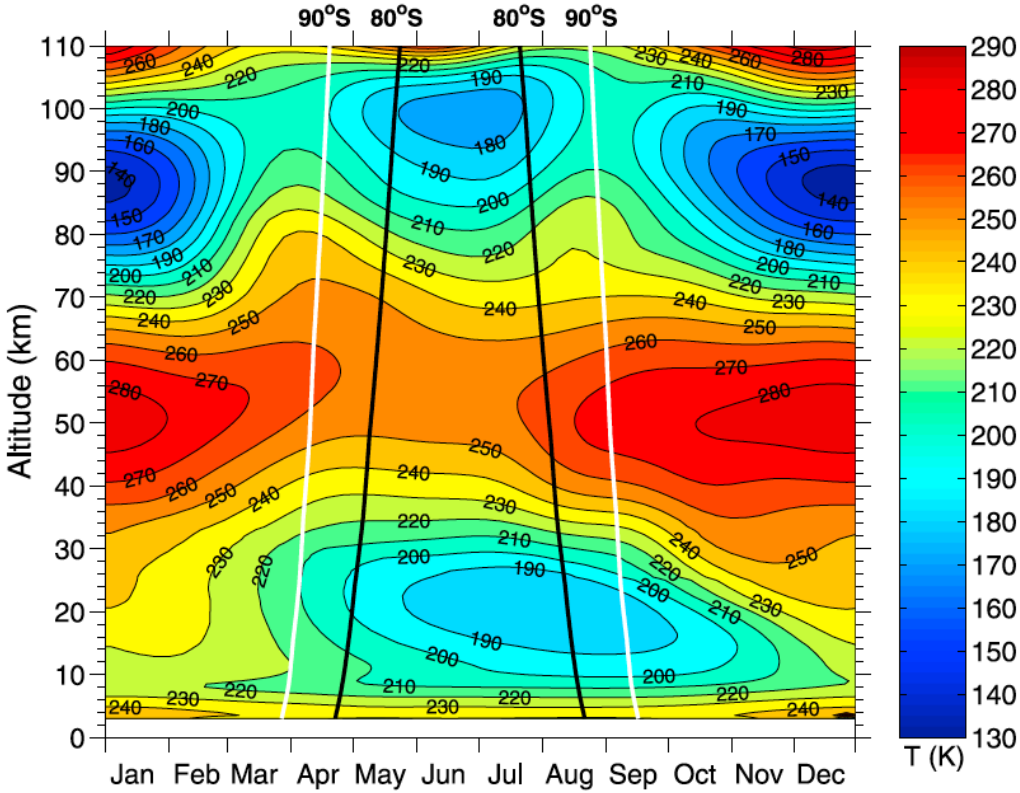

Figure 4. The observed weekly mean temperature structure of the atmosphere above South Pole (UISP-02) plotted from 3 to 110 km. Polar nights (24 h darkness) occur between the white curves at 90°S and between the black curves at 80°S. The vertical resolution is 500 m.

[Pan and Gardner, JGR, 2003]

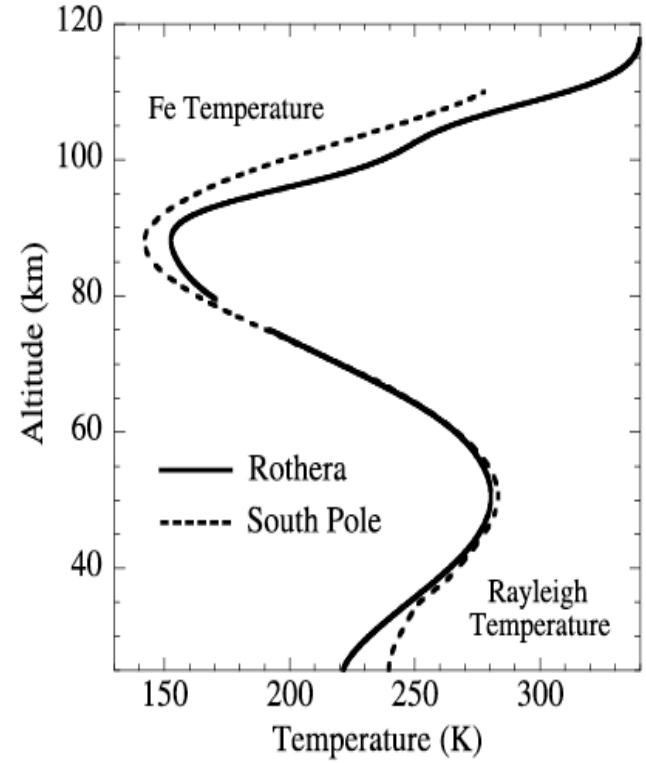

[Chu et al., GRL, 2004]

Utah State University Rayleigh Lidar

- Doubled Nd:YAG laser at 532 nm (630 mJ/pulse, 30 Hz)

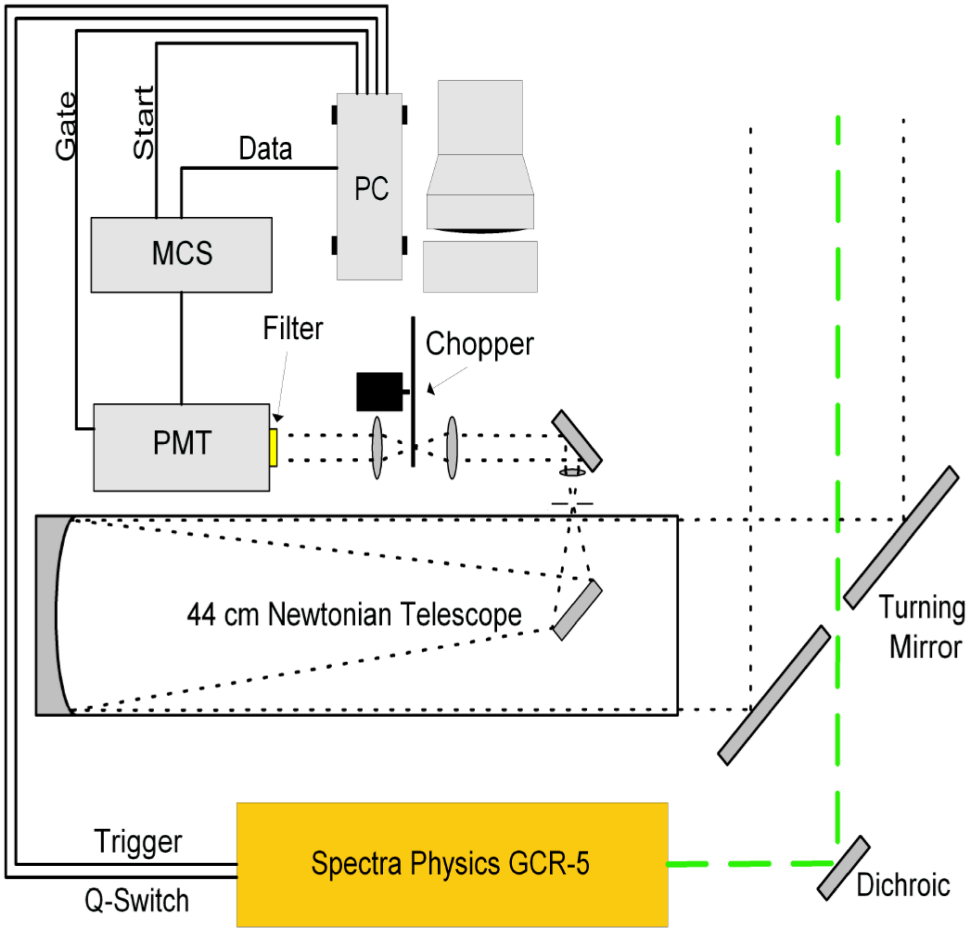

http://www.usu.edu/alo/aboutlidar.htm

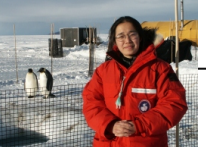

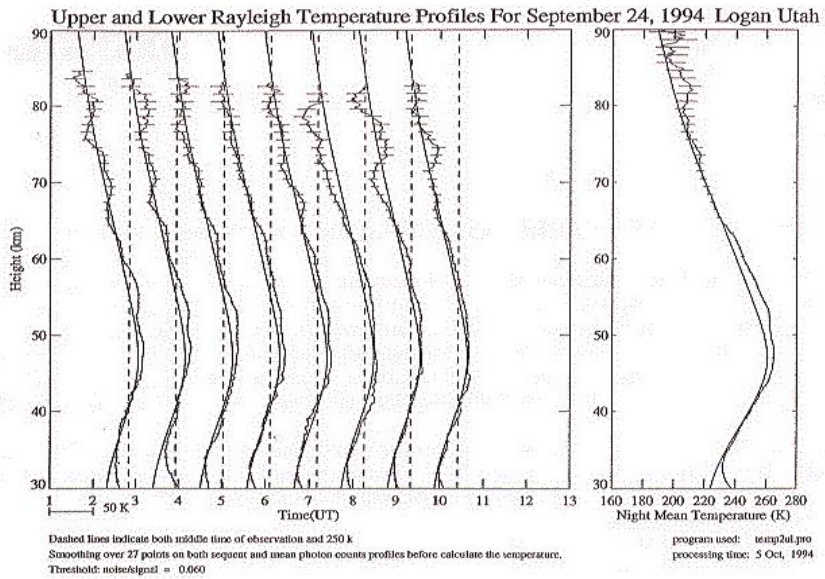

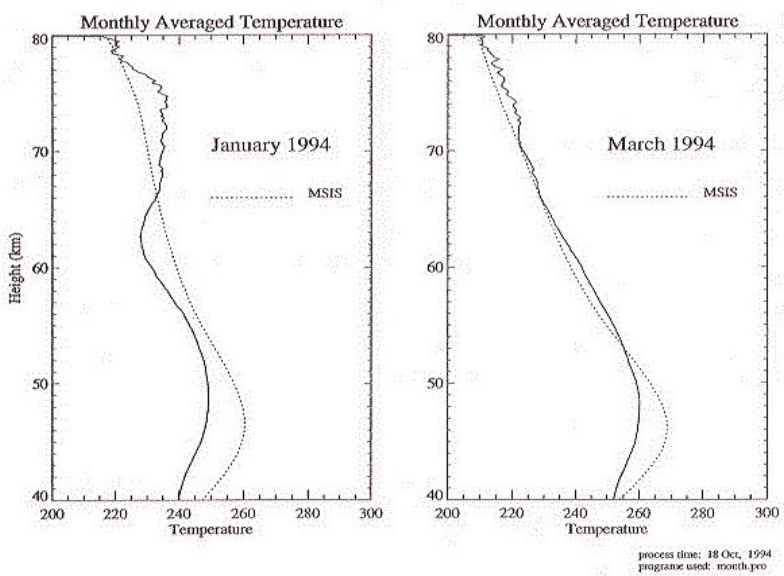

Sample Results from USU Rayleigh Lidar

Prof. Vincent Wickwar
& Josh Herron @ USU

http://www.usu.edu/alo/aboutlidar.htm

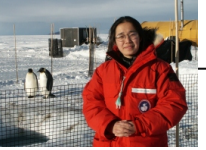

Greenland Rayleigh Lidar and Sample Results

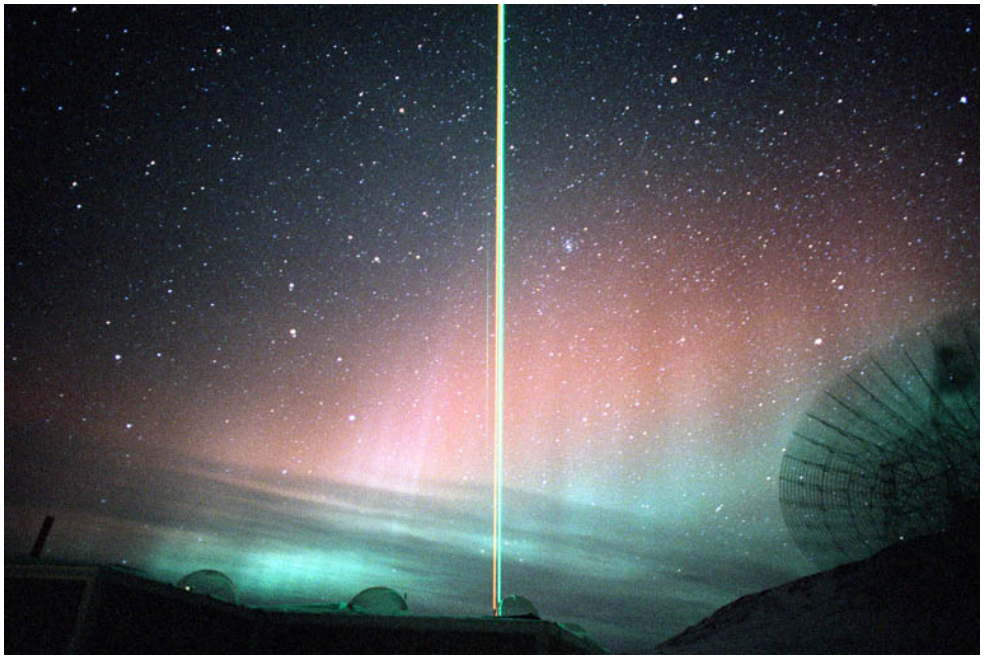

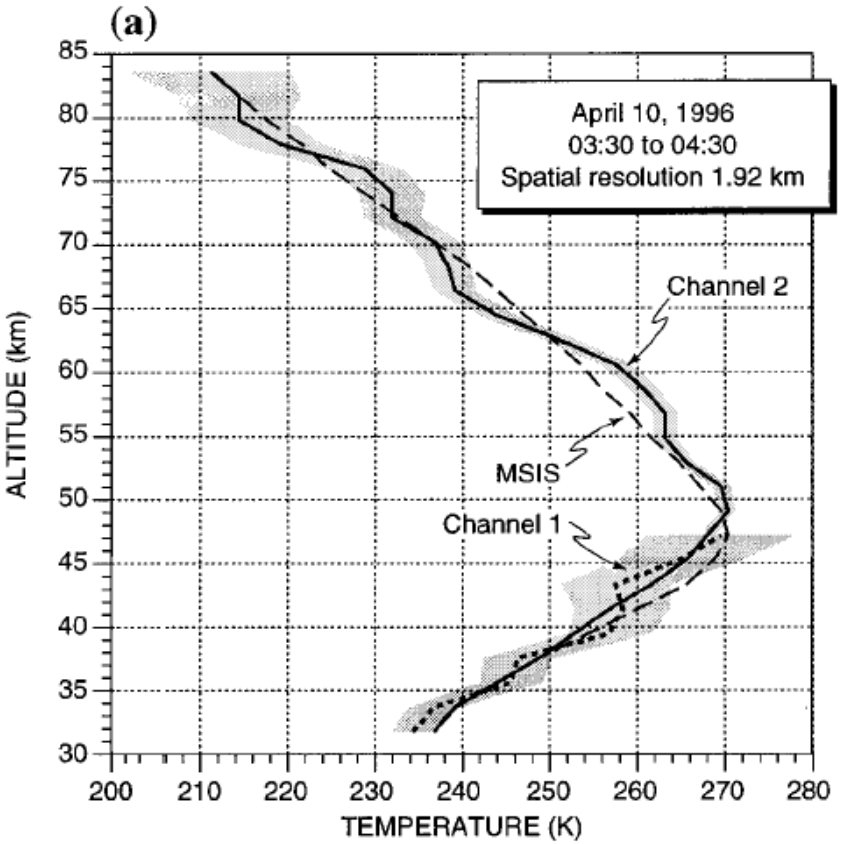

Courtesy of Jeff Thayer

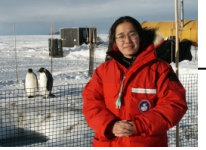

Greenland Rayleigh Lidar System

- The splitting of 5% and 95% Rayleigh signals helps resolve detector dynamic range issues, but requiring more photo detectors and calibrations.

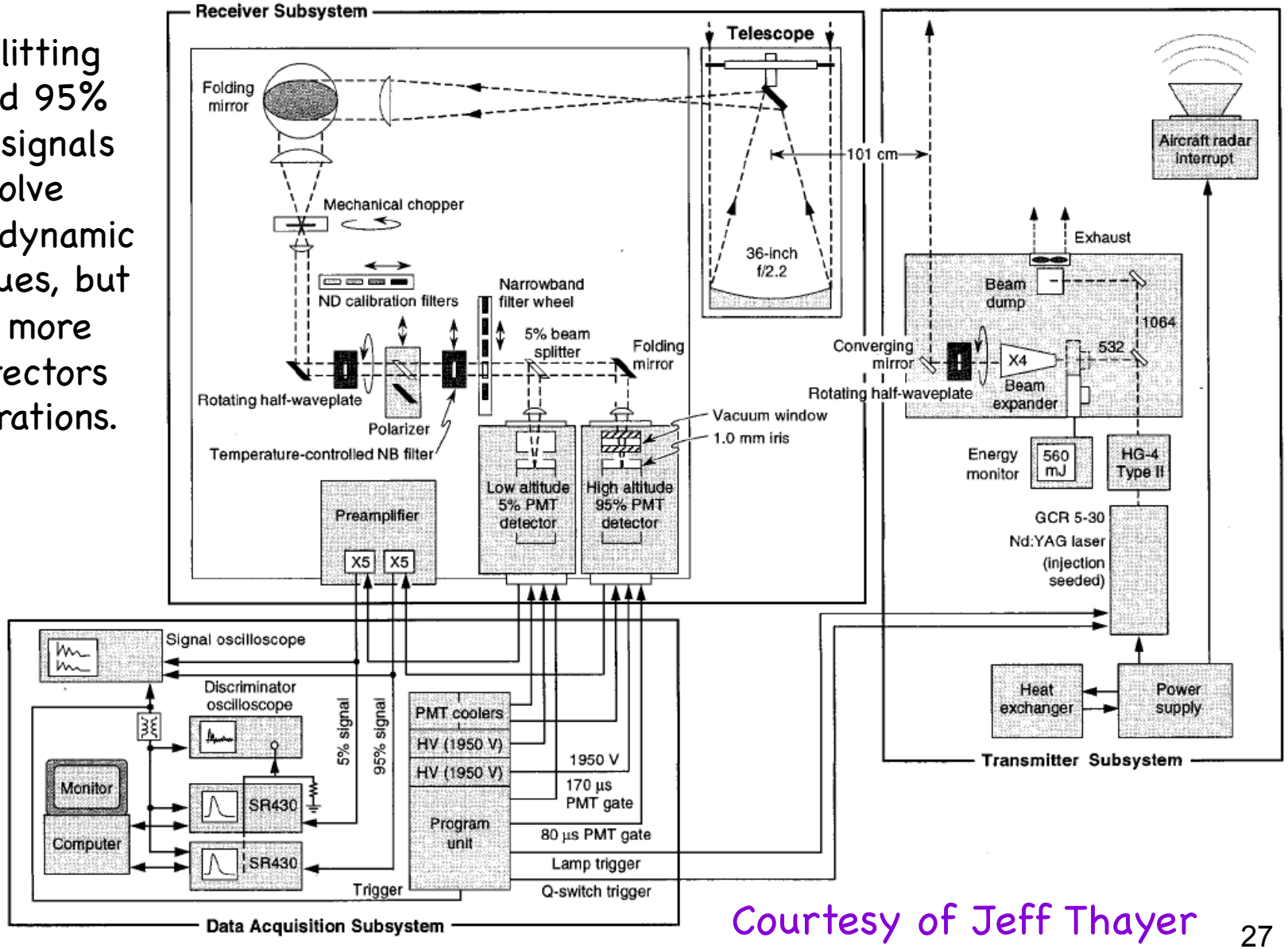

Courtesy of Jeff Thayer

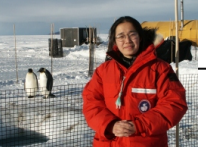

Non-Integration Temperature Techniques Near Boundary Layers

- Integration techniques require the ratio of return signals between different altitudes. Consequently, aerosol extinction effects cannot be cancelled out when aerosols dominate and vary dramatically with altitude, making integration lidars inadequate for the very lower atmosphere.
- A way to overcome this limitation is to employ techniques that don't require ratios among different altitudes but taking ratios at the same altitude but among different wavelengths or frequencies. Thus, most of aerosol effects can be cancelled out and temperature can be derived reliably.
- There could be various options. Here we present two options: One is the pure-rotational Raman Boltzmann technique, and another is the vibrational-rotational Raman Doppler technique.
- Unfortunately, none of these two alternatives is easy to implement as they demand very high-resolution filters.

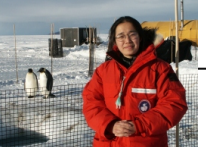

VR Raman Doppler Lidar Technique

532 nm

607 nm

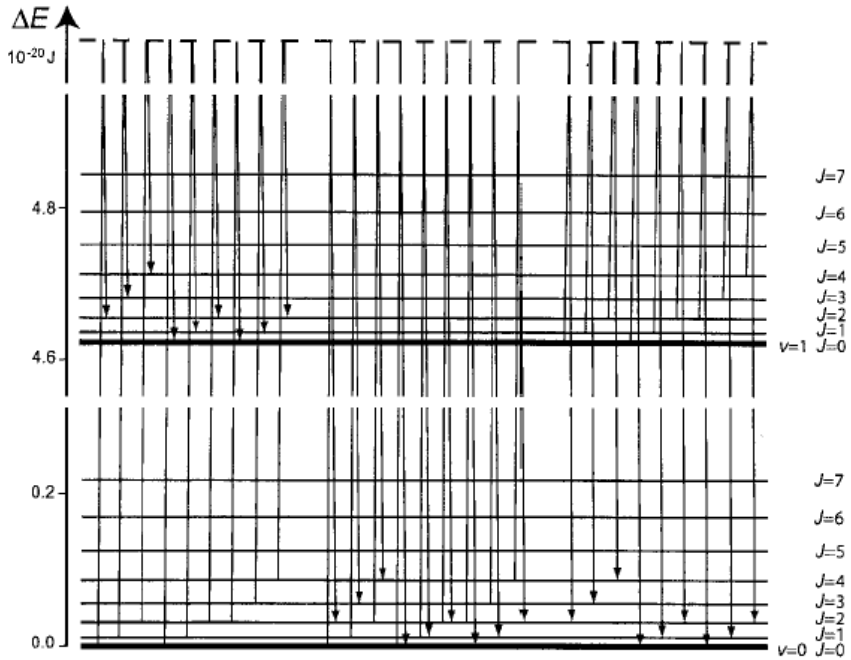

355 nm

387 nm

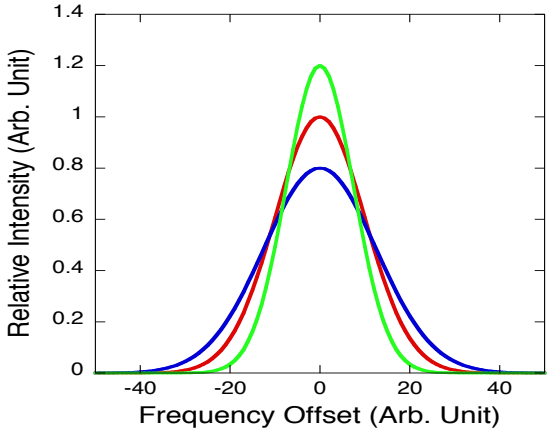

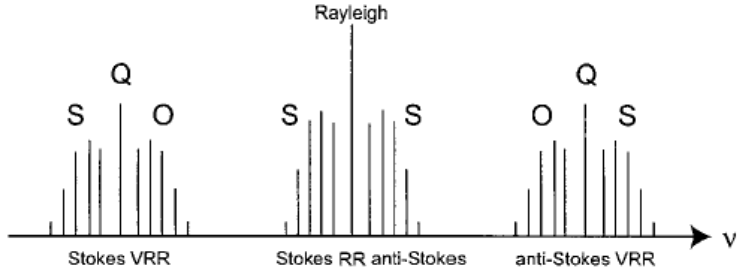

Taking the Q-branch of Stokes VR Raman & measuring its Doppler broadening to infer temperatures near boundary layers

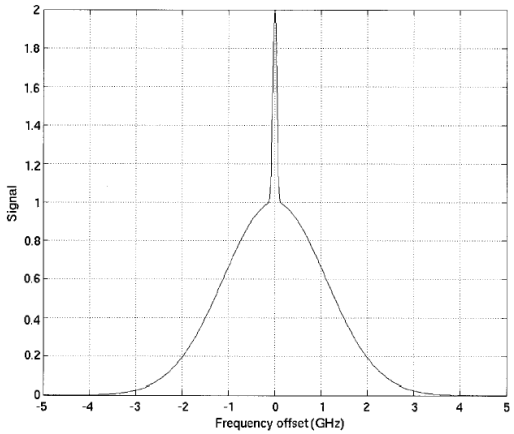

- Aerosol scattering disappears from VR Raman scattering signal.

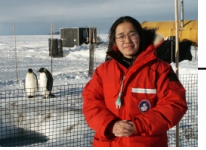

Pure-Rotational Raman Scattering

- Volume backscatter coefficient for single Raman lines

$$\beta_J(z) = \left(\frac{d\sigma}{d\Omega}\right)_J^{RR,VRR} n_J(z) = k_{\tilde{\nu}}\left(\tilde{\nu}_1 \mp |\Delta\tilde{\nu}|\right)^4 \frac{g_N \Phi_J}{(2I+1)Q} n(z) \exp\left[-\frac{B_i h c_0 J(J+1)}{k_B T}\right]$$

Which is the product of the transition probability and the population on the initial energy state. So the temperature dependence comes from the population distribution - Boltzmann distribution law!

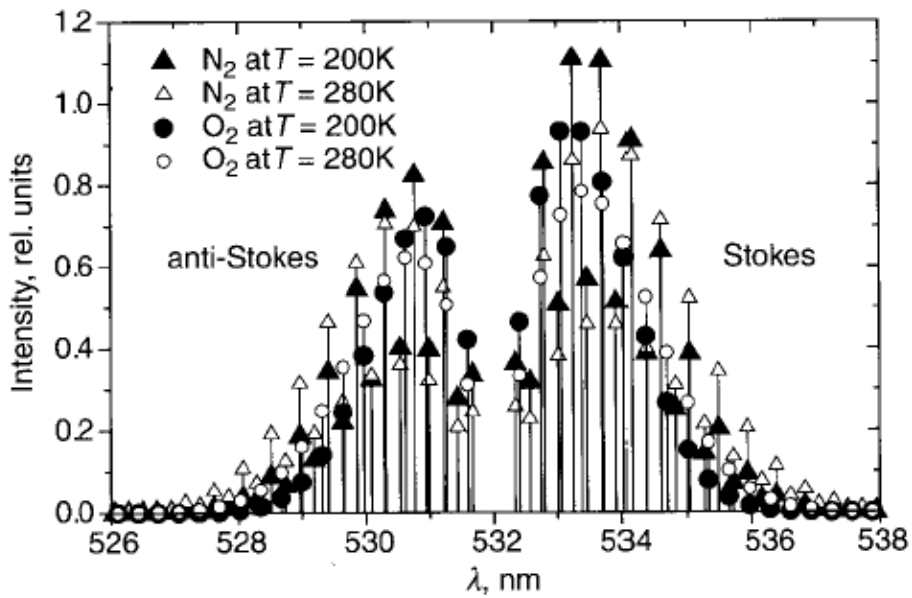

[Behrendt, "Temperature measurements with lidar", Chapter 10 in "Lidar", 2005]

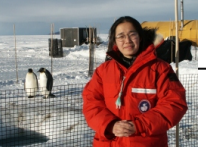

Rotational Raman Boltzmann Lidar

- Depending on what the initial energy state is, the line intensity can increase or decrease when temperature increases.
- If the initial energy state is one of the upper levels of the ground state, increasing in temperature will increase the population on the initial state, so the Raman line intensity will increase.
- If the initial energy state is the lowest level of the ground state, increasing temperature will decrease the population on the initial state, so the Raman line intensity will decrease.
- By measuring the intensity of two Raman lines with opposite temperature dependence, the ratio of these two lines is a sensitive function of atmospheric temperature.

$$Q(T, z) = \frac{S_{\mathrm{RR2}}(T, z)}{S_{\mathrm{RR1}}(T, z)}$$

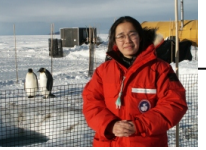

Rotational Raman Boltzmann Lidar

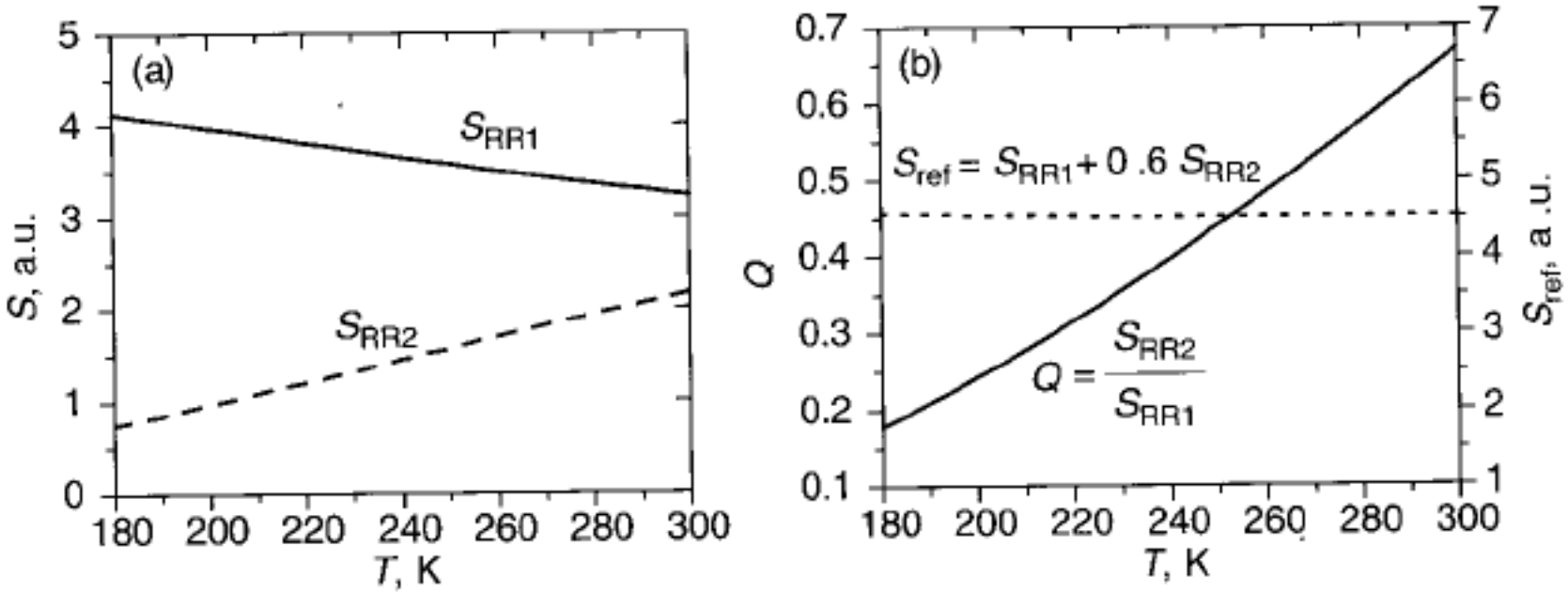

$$Q(T) = \frac{\sum_{i=O_2,N_2} \sum_{J_i} \tau_{RR2}(J_i)\eta_i \left(\frac{d\sigma}{d\Omega}\right)_{\pi}^{RR,i}(J_i)}{\sum_{i=O_2,N_2} \sum_{J_i} \tau_{RR1}(J_i)\eta_i \left(\frac{d\sigma}{d\Omega}\right)_{\pi}^{RR,i}(J_i)}$$

- Therefore, temperature can be derived from the ratio of two pure Rotational Raman line intensity. This is essentially the same principle as Boltzmann temperature technique!

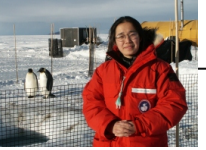

How Does Rotational Raman Tech Deal with Aerosol Extinction?

- Inelastic scattering – Raman scattering from air molecules

$$N_S(\lambda,\lambda_L,z) = \left(\frac{P_L(\lambda_L)\Delta t}{hc/\lambda_L}\right)\left(\sigma_{Raman}(\lambda_L,\lambda,z)n_{N_2}(z)\Delta z\right)\left(\frac{A}{z^2}\right)$$
$$\times \exp\left[-\int_0^z\left(\alpha_{aer}(\lambda_L,z')\right)dz'\right]\exp\left[-\int_0^z\left(\alpha_{aer}(\lambda,z')\right)dz'\right]$$
$$\times \exp\left[-\int_0^z\left(\alpha_{Ray}(\lambda_L,z')\right)dz'\right]\exp\left[-\int_0^z\left(\alpha_{Ray}(\lambda,z')\right)dz'\right]$$
$$\times\left(\eta(\lambda_L)\eta(\lambda)G(z)\right) + N_B$$

- Aerosol extinction effects are cancelled out when taking ratios between two Raman lines at the same altitude z.

$$\frac{N_S(\lambda_1,z)-N_B}{N_S(\lambda_2,z)-N_B} = \frac{n_{N_2}(z)}{n_{N_2}(z)}\cdot\frac{\cancel{\exp\left[-\int_0^z\left(\alpha_{aer}(\lambda_L,z')\right)dz'\right]}\exp\left[-\int_0^z\left(\alpha_{aer}(\lambda_1,z')\right)dz'\right]}{\cancel{\exp\left[-\int_0^z\left(\alpha_{aer}(\lambda_L,z')\right)dz'\right]}\exp\left[-\int_0^z\left(\alpha_{aer}(\lambda_2,z')\right)dz'\right]} = \frac{n_{N_2}(z)}{n_{N_2}(z)}$$

- For pure-rotational Raman scattering, λ_1 and λ_2 are very close, so the aerosol extinctions for these two wavelengths are approximately equal, so can be cancelled out. Consequently, rotational Raman lidar can be used for temperature measurements in the very lower atmosphere.

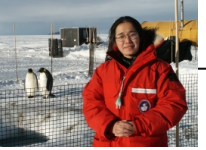

Technical Challenges in RR Boltzmann and VRR Doppler Lidars

- Rotational Raman (RR) temperature lidars are usually designed as add-on systems to existing lidar facilities, as RR lidars can share the same radiation sources with the existing lidars. This is because on frequency scale, the Raman shift is independent of laser wavelength.
- In principle, any lidar beam can generate rotational Raman scattering. So the major challenges to RR lidar are the high requirements on separation and blocking power of the filters implemented in the lidar receiver.
- The elastic scattering (Rayleigh and Mie) must be sufficiently compressed/eliminated, while the RR scattering lines with different temperature dependences must be separated from each other.
- Injection seeding to pulsed laser can help stabilize the laser output frequency, so helping the calibration of RR temperature lidar.
- Very narrowband filters (interference filters or others) are required and they must be stable in wavelength/frequency over time and usage. Due to the continuous advancement in filter and detector technologies, rotational Raman can be made reliable ...

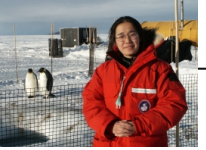

Technical Challenges in RR Boltzmann and VRR Doppler Lidars

- Vibrational-rotation Raman (VRR) Doppler lidars share the similar principles and techniques of Rayleigh Doppler lidar that will be discussed in later lectures. As long as we can manage to measure the Doppler broadening of the Q-branch Stokes VRR scattering, temperature can be inferred from the Doppler broadening.
- VRR Doppler lidar certainly demands extremely narrow (high-resolution) filters in order to infer the Doppler broadening. At the same time it also demands narrowband laser light with frequency either being very stable or stabilized to the narrowband filters.
- Basically whatever techniques that are applied to Rayleigh Doppler lidars can be applied to VRR Doppler lidars, e.g., various edge techniques, interferometers, fringe imaging, etc.

So far no one has ever demonstrated VRR Doppler lidar yet!

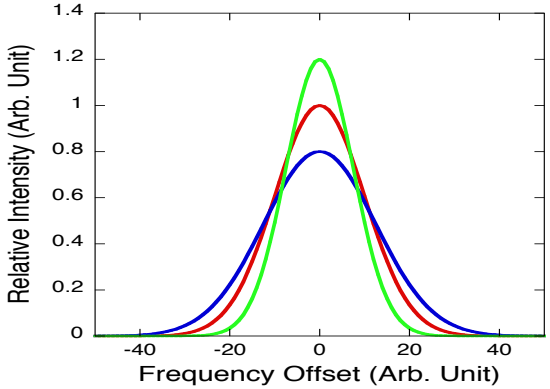

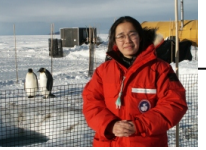

Results from Combined RR and Elastic Scattering Lidar

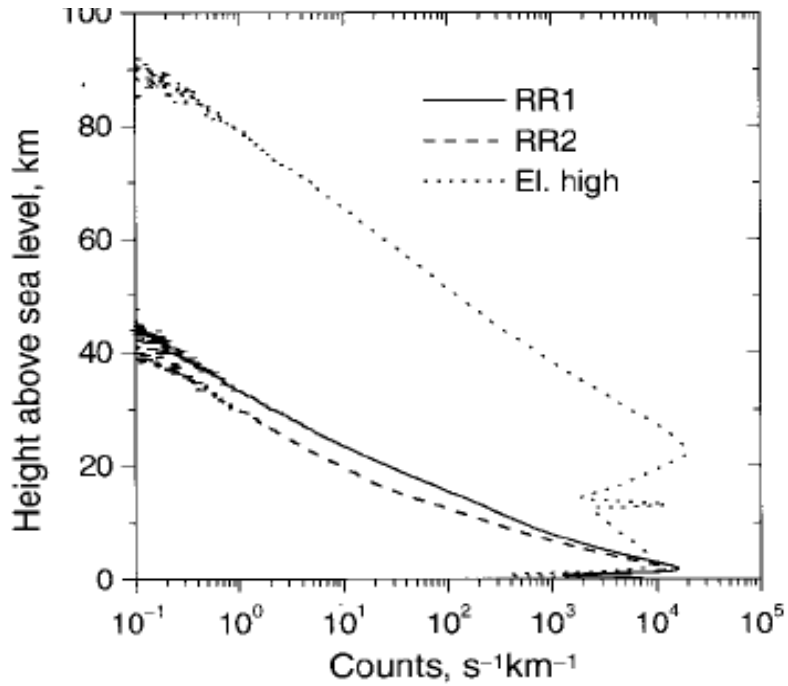

Fig. 10.11. Intensities of the RASC lidar signals for the temperature measurements: rotational Raman signals (RR1 and RR2) and high-altitude elastic signal (El. high). For this plot, 72 minutes (216,000 laser pulses) of nighttime lidar data were taken with a height resolution of 72 m, summed, the background was subtracted, and the data were finally smoothed with a sliding average of 360 m. The photon emission rate of the laser is $\sim 8 \times 10^{19}$ photons/s. In the high-altitude elastic signal, the effect of the chopper can be seen below ~25 km and the signature of a cirrus cloud in ~13 km height.

[Behrendt, "Temperature measurements with lidar", Chapter 10 in "Lidar", 2005]

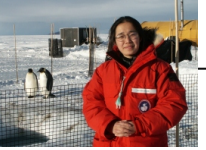

Results from Combined RR and Elastic Scattering Lidar

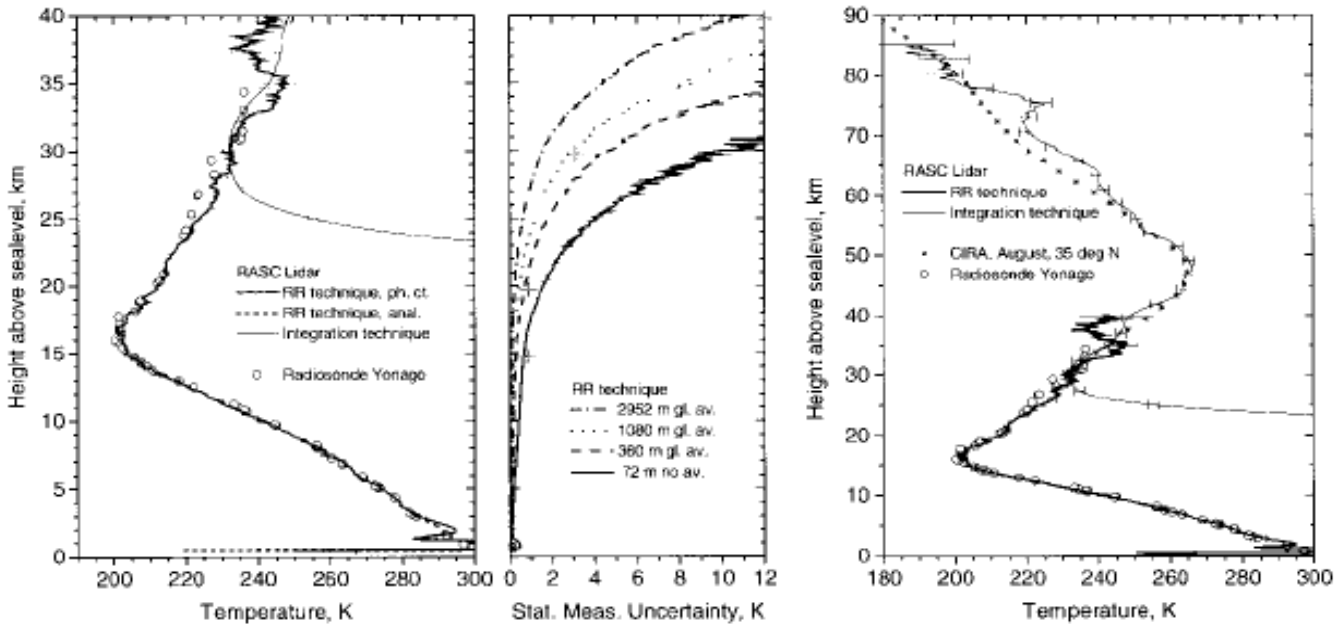

Fig. 10.12. Simultaneous temperature measurements with rotational Raman technique and with integration technique (signals see Fig. 10.11). Profiles of a climatological model atmosphere (CIRA-86 for 35°N and the month of the lidar measurements) and of a radiosonde are shown for comparison. Rotational Raman temperature data: height resolution of 72 m up to 15 km height, 360 m between 15 and 20 km height, 1080 m between 20 and 30 km height, and 2952 m above 30 km. Height resolution of the integration technique data is 2952 m. Error bars show the $1-\sigma$ statistical uncertainty of the measurements [48].

[Behrendt, "Temperature measurements with lidar", Chapter 10 in "Lidar", 2005]

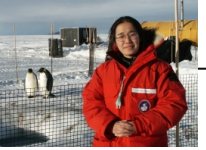

Summary

- Integration technique relies on the assumptions of hydrostatic equilibrium and ideal gas law in the atmosphere interested. It involves integrating the atmosphere relative density profile downward using a starting temperature (usually coming from a model or independent measurement) at an upper altitude.
- The key is to somehow measure the atmosphere relative number density with high precision and unbiased.
- Integration technique started with cw searchlight in 1950s, dramatically enhanced by high-power pulsed Rayleigh lidar in 1980s for region free of aerosols, further developed by vibrational Raman lidar in 1990s for region with aerosols. Inflatable falling sphere released by rocket is another perfect example for integration temperature technique.
- Pure-rotational Raman technique utilizes Boltzmann distribution to derive temperature in the lower atmosphere, while vibrational Raman Doppler technique utilizes Doppler broadening to derive temperature. Both can cancel out most of aerosol effects at the same altitudes, but put high demands on instrumentation – very narrowband filters.